



## FORCES IN DOUBLER TYPE SHEET CURRENT DIPOLES

S.C. Snowdon

March 22, 1974

Summary

The force distribution on a current sheet that simulates the current density distribution in the energy doubler dipole is calculated. For a perfectly centered dipole the magnetic forces result in a compressive force vertically and an elongative force horizontally. Net forces and torques on displaced current distribution are also calculated. Results are given for the dual test dipole, the doubler dipole, and the muon beam line dipole.

Magnetic Field

In complex variable notation, the magnetic field is given by

$$\begin{aligned}
 H^* = & -2ii_0 a \int_{-\frac{\pi}{2}}^{\frac{\pi}{2}} \left[ \frac{1}{z - \delta - \Delta - ae^{i\theta}} + \frac{1}{z - \frac{b^2}{\delta^* + \Delta + ae^{-i\theta}}} \right] \cos\theta d\theta \\
 & -2ii_0 a \int_{\frac{\pi}{2}}^{\frac{3\pi}{2}} \left[ \frac{1}{z - \delta + \Delta - ae^{i\theta}} + \frac{1}{z - \frac{b^2}{\delta^* - \Delta + ae^{-i\theta}}} \right] \cos\theta d\theta
 \end{aligned} \tag{1}$$

where it is assumed that the sheet current density is  $i_0 \cos\theta$ . Figure 1 should be consulted for geometrical quantities. If one designates  $s = e^{i\theta}$  then

$$\begin{aligned}
H^* = & -i_0 a \int_{C_1} \left[ \frac{1}{z-\delta-\Delta-as} + \frac{a+(\delta^*+\Delta)s}{az-[b^2-(\delta^*+\Delta)z]} \right] \left(1+\frac{1}{s^2}\right) ds \\
& -i_0 a \int_{C_2} \left[ \frac{1}{z-\delta+\Delta-as} + \frac{a+(\delta^*-\Delta)s}{az-[b^2-(\delta^*-\Delta)z]} \right] \left(1+\frac{1}{s^2}\right) ds. \quad (2)
\end{aligned}$$

Integration gives

$$\begin{aligned}
H^* = & -i_0 \left\{ -2\pi i - \ln \left( \frac{ia-z+\delta+\Delta}{ia+z-\delta-\Delta} \cdot \frac{ia+z-\delta+\Delta}{ia-z+\delta-\Delta} \right) \right. \\
& - \frac{a}{z-\delta-\Delta} \left[ -2i + \frac{a}{z-\delta-\Delta} \ln \left( \frac{ia-z+\delta+\Delta}{ia+z-\delta-\Delta} \right) \right] \\
& - \frac{a}{z-\delta+\Delta} \left[ 2i + \frac{a}{z-\delta+\Delta} \ln \left( \frac{ia+z-\delta+\Delta}{ia-z+\delta-\Delta} \right) \right] \\
& - \frac{2ia(\delta^*+\Delta)}{b^2-(\delta^*+\Delta)z} + \frac{2ia(\delta^*-\Delta)}{b^2-(\delta^*-\Delta)z} \\
& - \frac{a^2b^2}{[b^2-(\delta^*+\Delta)z]^2} \left[ i\pi + \ln \left( \frac{i[b^2-(\delta^*+\Delta)z]-az}{i[b^2-(\delta^*+\Delta)z]+az} \right) \right] \\
& - \frac{a^2b^2}{[b^2-(\delta^*-\Delta)z]^2} \left[ i\pi + \ln \left( \frac{i[b^2-(\delta^*-\Delta)z]+az}{i[b^2-(\delta^*-\Delta)z]-az} \right) \right] \\
& \left. - \frac{b^2}{z^2} \cdot \ln \left( \frac{i[b^2-(\delta^*+\Delta)z]-az}{i[b^2-(\delta^*+\Delta)z]+az} + \frac{i[b^2-(\delta^*-\Delta)z]+az}{i[b^2-(\delta^*-\Delta)z]-az} \right) \right\}
\end{aligned}$$

where the arguments of the logarithmic terms have been arranged so that the solution is appropriate to the inside region.

For  $z$  on the current sheet the field is discontinuous such that

$$H_t^+ - H_t^- = 4\pi i_0 \cos\theta, \quad H_n^+ = H_n^- \quad (4)$$

which yields

$$H^*(+) - H^*(-) = -4\pi i_0 \cos\theta e^{-i\theta}. \quad (5)$$

Hence the average field in the current sheet is

$$\langle H^* \rangle_{Av} = H^*(-) - i\pi i_0 (1 + e^{-2i\theta}). \quad (6)$$

### Force

If  $S_x$  and  $S_y$  designate stresses on a unit area of the current sheet, then

$$S^* = S_x - iS_y = -i\langle H^* \rangle_{Av} i_0 \cos\theta. \quad (7)$$

The net force per unit length of current sheet is then

$$F^* = \oint_c S^* ad\theta. \quad (8)$$

### Torque

The torque per unit length of the current sheet is

$$T_z = \text{Real} \left[ i \oint_c z S^* ad\theta \right]. \quad (9)$$

There can be no torque about the central axis since the iron shield is symmetrical about this axis. However, if  $z = \delta + z'$ , the origin of  $z'$  being center of the displaced bore tube then,

$$T_{z'} = \text{Real} \left[ i \oint_c z' S^* \, \text{ad}\theta \right]. \quad (10)$$

But

$$T_z = 0 = \text{Real} \left[ i \oint_c (\delta + z') S^* \, \text{ad}\theta \right]. \quad (11)$$

Hence

$$T_{z'} = - \text{Real} \left[ i \delta \oint_c S^* \, \text{ad}\theta \right] = - \text{Real} (i \delta F^*). \quad (12)$$

### Results

Application of the previous formulas using input data appropriate for the dual test dipole, the doubler dipole, and the muon beam line dipole gives the results shown in Tables (1-3).

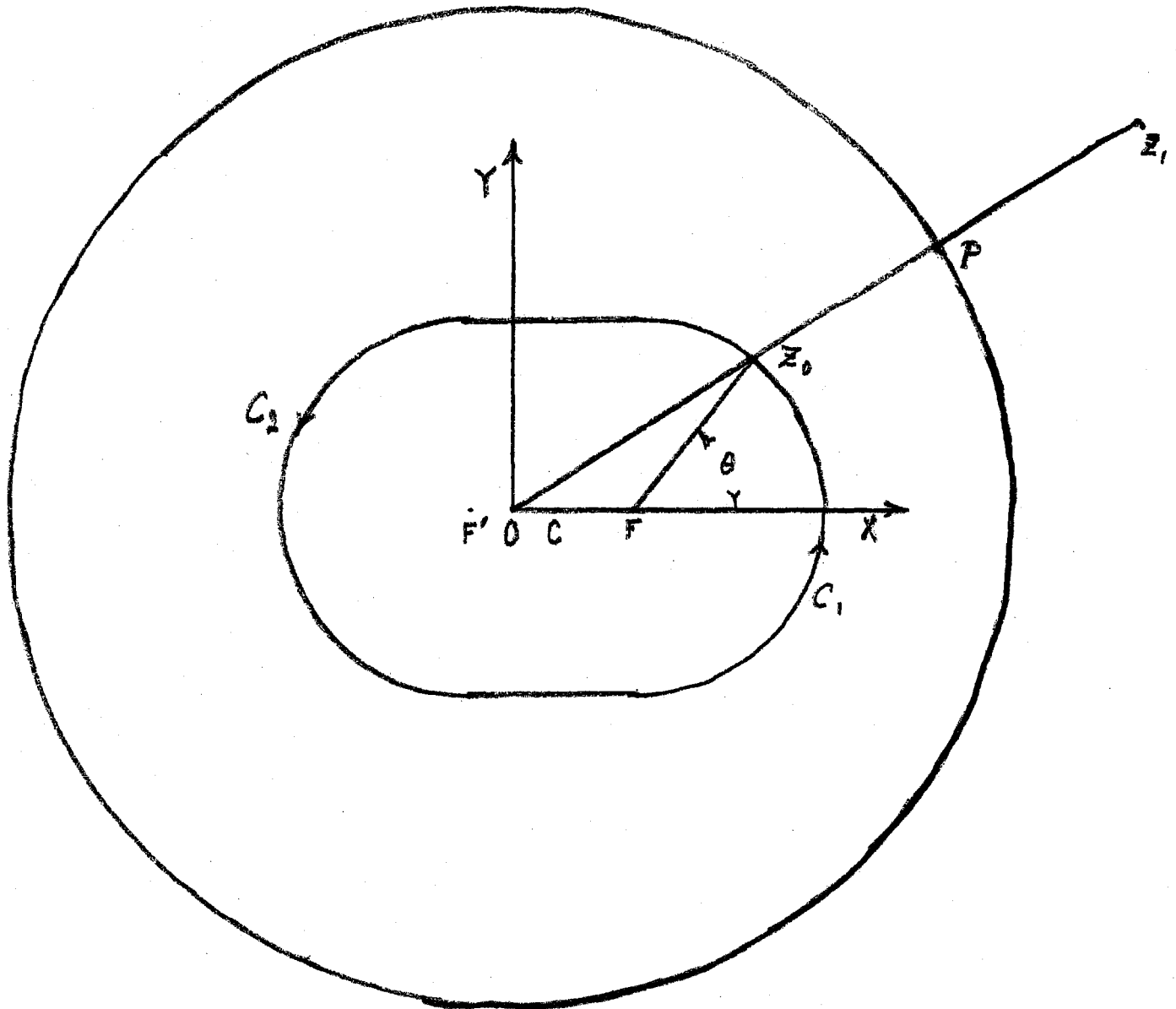


Figure 1. Sheet Current Dipole (See Legend)

Figure 1. Legend

O - Equilibrium Center

C - Displaced Center

F - Origin of Right Hand Circular Sheet Current

F' - Origin of Left Hand Circular Sheet Current

$z_1$  = Image Position of  $z_0$

a = Radius at Current Sheet (F- $z_0$ )

b = Inner Radius of Iron (O-P)

$\Delta$  = Offset (F'-C or C-F)

$\delta$  = Displacement of Bore Tube Center (O-C)

$$H^* = -2iI \left( \frac{1}{z-z_0} + \frac{1}{z-z_1} \right)$$

$$z_0 = \begin{cases} \delta + \Delta + ae^{i\theta} & \text{Right Hand Sheet} \\ \delta - \Delta + ae^{i\theta} & \text{Left Hand Sheet} \end{cases}$$

$$z_1 = \frac{b^2}{z_0^*}$$

$$I = i_0 a \cos \theta d\theta$$

Note that the origin of  $\theta$  is F for  $-\frac{\pi}{2} < \theta < \frac{\pi}{2}$  and F' for  $\frac{\pi}{2} < \theta < \frac{3\pi}{2}$

Table 1. Magnetic Stresses in Dual Test Dipole

|                      |          |
|----------------------|----------|
| Conductor Current    | 2625A    |
| Number of Conductors | 130      |
| Current Sheet Radius | 1.340 in |
| Current Sheet Offset | .000 in  |
| Inner Radius of Iron | 3.050 in |
| Central Field        | 37.6 kG  |
| Stress:              |          |

| Quadrant | Angle<br>(Deg) | X-Stress<br>(P/in/in) | Y-Stress<br>(P/in/in) |
|----------|----------------|-----------------------|-----------------------|
| 1        | 0              | 441                   | 0                     |
|          | 10             | 503                   | -385                  |
|          | 20             | 666                   | -691                  |
|          | 30             | 877                   | -858                  |
|          | 40             | 1062                  | -863                  |
|          | 50             | 1146                  | -724                  |
|          | 60             | 1078                  | -495                  |
|          | 70             | 842                   | -251                  |
|          | 80             | 462                   | -68                   |
|          | 90             | 0                     | 0                     |
| 2        | 90             | 0                     | 0                     |
|          | 100            | -462                  | -68                   |
|          | 110            | -842                  | -251                  |
|          | 120            | -1078                 | -495                  |
|          | 130            | -1146                 | -724                  |
|          | 140            | -1062                 | -863                  |
|          | 150            | -877                  | -858                  |
|          | 160            | -666                  | -691                  |
|          | 170            | -503                  | -385                  |
|          | 180            | -441                  | 0                     |

Table 1. (Cont.)

| Quadrant | Angle<br>(Deg) | X-Stress<br>(P/in/in) | Y-Stress<br>(P/in/in) |
|----------|----------------|-----------------------|-----------------------|
| 3        | 180            | -441                  | 0                     |
|          | 190            | -503                  | 385                   |
|          | 200            | -666                  | 691                   |
|          | 210            | -877                  | 858                   |
|          | 220            | -1062                 | 863                   |
|          | 230            | -1146                 | 724                   |
|          | 240            | -1078                 | 495                   |
|          | 250            | -842                  | 251                   |
|          | 260            | -462                  | 68                    |
|          | 270            | 0                     | 0                     |
| 4        | 270            | 0                     | 0                     |
|          | 280            | 462                   | 68                    |
|          | 290            | 842                   | 251                   |
|          | 300            | 1078                  | 495                   |
|          | 310            | 1146                  | 724                   |
|          | 320            | 1062                  | 863                   |
|          | 330            | 877                   | 858                   |
|          | 340            | 666                   | 691                   |
|          | 350            | 503                   | 385                   |
|          | 360            | 441                   | 0                     |

## Resultant Forces and Torque (about bore tube center)

| X-Displ.<br>(in) | Y-Displ.<br>(in) | X-Force<br>(P/in) | Y-Force<br>(P/in) | Z-Torque<br>(in·P/in) |
|------------------|------------------|-------------------|-------------------|-----------------------|
| .010             | .000             | 5.35              | .00               | .00                   |
| .000             | .010             | .00               | 5.35              | .00                   |
| .010             | .010             | 5.35              | 5.35              | .00                   |



Table 2. Magnetic Stresses in Doubler Dipole

|                      |           |
|----------------------|-----------|
| Conductor Current    | 2815A     |
| Number of Conductors | 140       |
| Current Sheet Radius | 1.1325 in |
| Current Sheet Offset | .375 in   |
| Inner Radius of Iron | 3.0625 in |
| Central Field        | 45.5 kG   |
| Stress:              |           |

| Quadrant | Angle<br>(Deg) | X-Stress<br>(P/in/in) | Y-Stress<br>(P/in/in) |
|----------|----------------|-----------------------|-----------------------|
| 1        | 0              | 534                   | 0                     |
|          | 10             | 651                   | -759                  |
|          | 20             | 965                   | -1367                 |
|          | 30             | 1374                  | -1710                 |
|          | 40             | 1740                  | -1743                 |
|          | 50             | 1925                  | -1497                 |
|          | 60             | 1832                  | -1069                 |
|          | 70             | 1431                  | -596                  |
|          | 80             | 775                   | -210                  |
|          | 90             | 0                     | 0                     |
| 2        | 90             | 0                     | 0                     |
|          | 100            | -775                  | -210                  |
|          | 110            | -1431                 | -596                  |
|          | 120            | -1832                 | -1069                 |
|          | 130            | -1925                 | -1497                 |
|          | 140            | -1740                 | -1743                 |
|          | 150            | -1374                 | -1710                 |
|          | 160            | -965                  | -1367                 |
|          | 170            | -651                  | -759                  |
|          | 180            | -534                  | 0                     |

Table 2. (Cont.)

TM-483  
0428

| Quadrant | Angle<br>(Deg) | X-Stress<br>(P/in/in) | Y-Stress<br>(P/in/in) |
|----------|----------------|-----------------------|-----------------------|
| 3        | 180            | -534                  | 0                     |
|          | 190            | -651                  | 759                   |
|          | 200            | -965                  | 1367                  |
|          | 210            | -1374                 | 1710                  |
|          | 220            | -1740                 | 1743                  |
|          | 230            | -1925                 | 1497                  |
|          | 240            | -1832                 | 1069                  |
|          | 250            | -1431                 | 596                   |
|          | 260            | -775                  | 210                   |
|          | 270            | 0                     | 0                     |
| 4        | 270            | 0                     | 0                     |
|          | 280            | 775                   | 210                   |
|          | 290            | 1431                  | 596                   |
|          | 300            | 1832                  | 1069                  |
|          | 310            | 1925                  | 1497                  |
|          | 320            | 1740                  | 1743                  |
|          | 330            | 1374                  | 1710                  |
|          | 340            | 965                   | 1367                  |
|          | 350            | 651                   | 759                   |
|          | 360            | 534                   | 0                     |

Resultant Force and Torque (about bore tube center)

| X-Displ.<br>(in) | Y-Displ.<br>(in) | X-Force<br>(P/in) | Y-Force<br>(P/in) | Z-Torque<br>(in·P/in) |
|------------------|------------------|-------------------|-------------------|-----------------------|
| .010             | .000             | 11.04             | .00               | .00                   |
| .000             | .010             | .00               | 9.48              | .00                   |
| .010             | .010             | 11.04             | 9.48              | .0156                 |

Table 3. Magnetic Stresses in Muon Line Dipole

|                      |          |
|----------------------|----------|
| Conductor Current    | 2380A    |
| Number of Conductors | 306      |
| Current Sheet Radius | 2.489 in |
| Current Sheet Offset | 1.000 in |
| Inner Radius of Iron | 5.750 in |
| Central Field        | 40.5 kG  |
| Stress:              |          |

| Quadrant | Angle<br>(Deg) | X-Stress<br>(P/in/in) | Y-Stress<br>(P/in/in) |
|----------|----------------|-----------------------|-----------------------|
| 1        | 0              | 642                   | 0                     |
|          | 10             | 719                   | -548                  |
|          | 20             | 926                   | -988                  |
|          | 30             | 1191                  | -1237                 |
|          | 40             | 1419                  | -1264                 |
|          | 50             | 1514                  | -1089                 |
|          | 60             | 1410                  | -782                  |
|          | 70             | 1088                  | -440                  |
|          | 80             | 585                   | -160                  |
|          | 90             | 0                     | 0                     |
| 2        | 90             | 0                     | 0                     |
|          | 100            | -585                  | -160                  |
|          | 110            | -1088                 | -440                  |
|          | 120            | -1410                 | -782                  |
|          | 130            | -1514                 | -1089                 |
|          | 140            | -1419                 | -1264                 |
|          | 150            | -1191                 | -1237                 |
|          | 160            | -926                  | -988                  |
|          | 170            | -719                  | -548                  |
|          | 180            | -642                  | 0                     |

Table 3. (Cont.)

TM-483  
0428

| Quadrant | Angle<br>(Deg) | X-Stress<br>(P/in/in) | Y-Stress<br>(P/in/in) |
|----------|----------------|-----------------------|-----------------------|
| 3        | 180            | -642                  | 0                     |
|          | 190            | -719                  | 548                   |
|          | 200            | -926                  | 988                   |
|          | 210            | -1191                 | 1237                  |
|          | 220            | -1419                 | 1264                  |
|          | 230            | -1514                 | 1089                  |
|          | 240            | -1410                 | 782                   |
|          | 250            | -1088                 | 440                   |
|          | 260            | -585                  | 160                   |
|          | 270            | 0                     | 0                     |
| 4        | 270            | 0                     | 0                     |
|          | 280            | 585                   | 160                   |
|          | 290            | 1088                  | 440                   |
|          | 300            | 1410                  | 782                   |
|          | 310            | 1514                  | 1089                  |
|          | 320            | 1419                  | 1264                  |
|          | 330            | 1191                  | 1237                  |
|          | 340            | 926                   | 988                   |
|          | 350            | 719                   | 548                   |
|          | 360            | 642                   | 0                     |

Resultant Force and Torque (about bore tube center)

| X-Displ.<br>(in) | Y-Displ.<br>(in) | X-Force<br>(P/in) | Y-Force<br>(P/in) | Z-Torque<br>(in·P/in) |
|------------------|------------------|-------------------|-------------------|-----------------------|
| .010             | .000             | 17.82             | .00               | .00                   |
| .000             | .010             | .00               | 13.70             | .00                   |
| .010             | .010             | 17.82             | 13.70             | .0412                 |